Photoelastic trends for amorphous and crystalline solids of differing network dimensionality

B. A. Weinstein, R. Zallen, and M. L. Slade
Xerox Webster Research Center, Webster, New York 14580

A. deLozanne*
Purdue University, West Lafayette, Indiana 47907
(Received 29 May 1981)

A single model is developed for the different photoelastic response of Ge-family materials and chalcogen-based molecular solids. If χ' is the "Grüneisen" parameter for the electronic susceptibility, experiment shows that $\chi'<0$ for the former group, while $\chi'>1$ for the latter. In addition, several group IV-VI compounds have $0\leq\chi'\leq 1$. In our model the dielectric constant is calculated, within the Drude formalism, using one Penn-Phillips oscillator for Ge-family solids and two for molecular chalcogenides. The model predicts that χ' should depend linearly on $2\eta/E_g$, with E_g the Penn-Phillips gap and dimensionless η determined from experiment. Reliable values of χ', E_g, and other relevant parameters are tabulated for a large number of materials. New experimental results are also presented for ZnTe. The experimental evidence provides support for the model. A plot of χ' versus $2\eta/E_g$ exhibits the predicted linear correlations for materials with $\chi'<0$ and $\chi'>1$; the slopes are in excellent agreement with measured band-gap volume derivatives. These correlations pertain to amorphous and crystalline solids alike. For the molecular chalcogenides, it is concluded that band-broadening influences χ' through a uniform "red shift" of the lower-energy oscillator with respect to the stationary upper oscillator. The observed photoelastic trends are related to bonding topology by analogy with arguments previously applied to phonons. $\chi'>1$ follows from the bonding strength dichotomy in ($<$3D)-network structures, whereas $\chi'<0$ obtains for covalent 3D-network solids. It is suggested that χ' can serve as an indicator of network dimensionality for these two cases.

I. INTRODUCTION

The effect of compression on the low-frequency optical dielectric constant of nonmetallic solids ($\epsilon_0=n_0^2$, where n_0 is the infrared refractive index in the transparent regime) has been treated by many authors.[1-7] For ionic solids,[1] especially the alkali halides, the Lorenz-Lorentz local-field formalism has often been applied. However, substantial pressure-induced changes in the ionic polarizability must be included in many cases.[8,9] Van Vechten[2] showed that, within the Drude formalism, a Penn-Phillips—type single-oscillator model[10,11] could successfully treat covalent and ionic A^NB^{8-N} crystals. In particular, Van Vechten could explain the qualitatively different behavior of covalent Ge-family (groups IV, III—V, and II—VI) semiconductors, and the alkali halides. This difference is reflected in the sign of the photoelastic parameter χ' defined by

$$\chi'=-\frac{d\ln\chi}{d\ln V}\ , \tag{1}$$

where $\chi=(\epsilon_0-1)/4\pi$ is the electronic susceptibility. One finds that $\chi'<0$ for Ge-family materials, and $\chi'>0$ for alkali halides.

The tetrahedral structure of the Ge family constitutes a covalently bonded macroscopically three-dimensional (3D) network. We shall also be concerned here with solids characterized by covalently bonded networks of macroscopic dimensionality less than 3.[12,13] Typical examples are layered As_2S_3 (2D network), chainlike trigonal Se (1D network), and orthorhombic S (0D network, consisting of isolated S_8 rings). As a consequence of low network dimensionality, these chalcogen-based materials (materials containing a high concentration of group VI atoms) can be classified as molecular solids.[12,13]

The photoelastic behavior of these molecular chalcogenides presents an even more striking con-

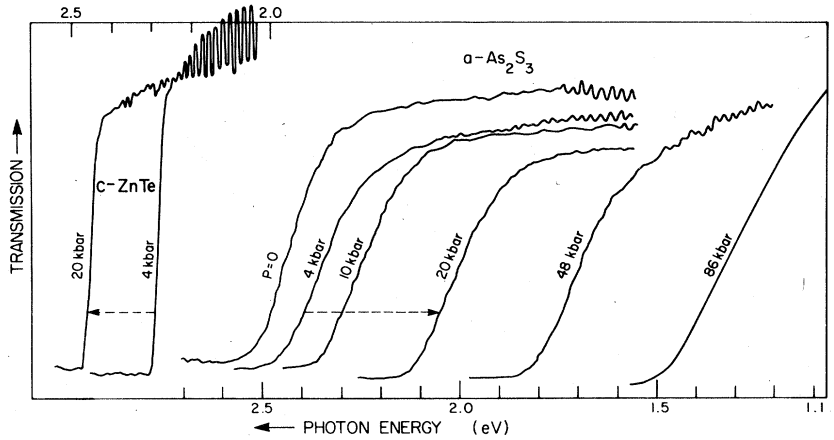

FIG. 1. Effect of pressure (room temperature) on the transmission edges (absorptions $\alpha \sim 10^2 - 10^4$ cm^{-1}) of c-ZnTe and a-As_2S_3. Note, photon energy increase to the left. Upper and lower scales pertain to c-ZnTe and a-As_2S_3, respectively. The blue shift for c-ZnTe and red shift for a-As_2S_3 between 4 and 20 kbar are emphasized by dashed arrows. The a-As_2S_3 edge does not broaden substantially until the pressure medium becomes quasihydrostatic, ~ 90 kbar. The sharper c-ZnTe edge broadens markedly at ~ 65 kbar, presumably becoming indirect due to the crossover of Γ and X gaps. Optical path length $n_0 d$ at each pressure was determined from the fringe spacing in the transparent region, at ~ 1.75 eV for c-ZnTe, and ~ 1.45 eV for a-As_2S_3.

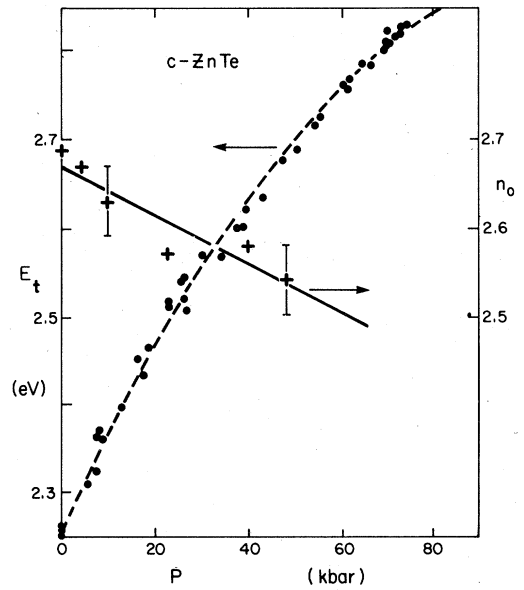

FIG. 2. Pressure dependence of refractive index n_0 at ~ 1.75 eV (crosses and solid line), and threshold energy E_t at $\alpha \simeq 5 \times 10^3$ cm^{-1} (solid circles and dashed curve), for c-ZnTe. Note contrast with Fig. 3. Sample thickness was $d = 11$ μm for n_0 measurements. Several samples (from the same starting material) of thicknesses $10-30$ μm were used to measure E_t. Sufficient data were recorded in overlapping pressure regions in order to accurately combine results. The best quadratic fit gave $E_t = (2.255 \pm 0.005)$ eV $+ (11.5 \pm 0.5) \times 10^{-3}$ eV/kbar $P - (5.0 \pm 0.3) \times 10^{-5}$ eV/kbar$^2 P^2$. Sublinear behavior above 65 kbar is due in part to the direct-indirect ($\Gamma - X$) edge crossover. A transition to a visibly opaque phase was observed at 95 ± 5 kbar.

trast to that of the Ge family than the behavior of the alkali halides. An excellent example of this can be seen in Figs. 1–3, which illustrate the pressure dependence of n_0 and the threshold band gap E_t of crystalline (c) ZnTe and amorphous (a) As_2S_3.[14,15] For c-ZnTe, E_t increases strongly with pressure, and n_0 decreases. The detailed depen-

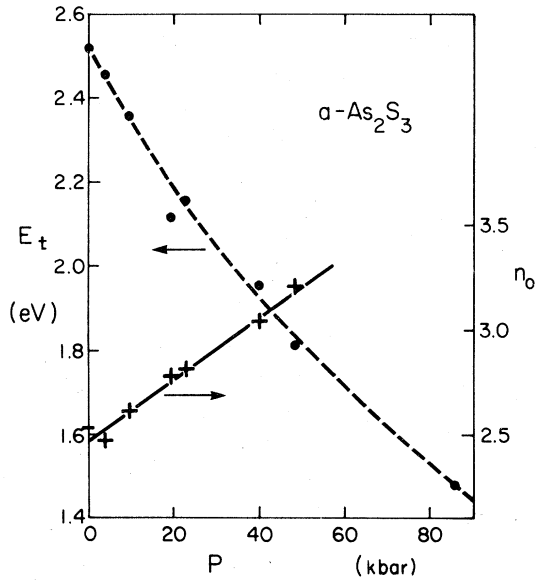

FIG. 3. Pressure dependence of refractive index n_0 at ~ 1.45 eV (crosses and solid line), and threshold energy E_t at $\alpha \simeq 5 \times 10^3$ cm^{-1} (solid circles and dashed curve), for a-As_2S_3. Note contrast with Fig. 2.

dences are shown in Fig. 2. [The data shown here for c-ZnTe are new, and were obtained by us in hydrostatic-pressure experiments using the ruby-calibrated diamond-anvil-cell technique.[16] The initial ($P=0$) band-gap coefficient dE_t/dP agrees well with an earlier low-pressure result,[17] and our results for dn_0/dP are the first reported for this material. The pressure dependence of the refractive index was obtained from the interference-fringe spacing in the transparent region (see Fig. 1).] In contrast, Fig. 3 shows that for a-As_2S_3, E_t has an even stronger "red shift" to lower energy, whereas n_0 increases rapidly with pressure. In fact, for a-As_2S_3 and many other molecular solids of low network dimensionality (<3D), χ' is not only positive, but unlike the alkali halides,[2] χ' is substantially greater than 1.

Kastner[5] studied the effect of pressure on several chalcogenide glasses and crystals, and applied the Lorenz-Lorentz formalism to his results. The local-field correction, initially believed to be substantial,[5] was subsequently shown to be small.[6] Connell and Paul[4] studied the pressure dependence of ϵ_0 and E_t for amorphous and crystalline Si, Ge, GaP, and GaAs. They found χ' nearly the same for the amorphous and crystalline forms, and concluded that the average Penn-Phillips gap E_g, had been unaffected by the disorder. However, they found $dE_t/dP < dE_g/dP$ in the disordered solids, contrary to the situation in crystals. They interpreted this as evidence against the virtual crystal model as a description of band-edge states in amorphous III—V materials. Building on the observation that $dE_t/dP < dE_g/dP$ in amorphous Si, Ge, GaP, and GaAs, Lucovsky[7] treated the photoelastic behavior of chalcogenide glasses under the ansatz $d\ln E_t/dP = d\ln E_g/dP$. Applying the Penn-Phillips model, he obtained reasonable agreement for Se, As_2Se_3, $GeSe_2$, and As_2S_3. For reasons to be mentioned below, we question his underlying assumption.

In the present work our attention centers around the different photoelastic response of covalent 3D-network materials, and molecular solids of lower network dimensionality.[12] Stated succinctly, we serve that $\chi'<0$ for the former and $\chi'>1$ for the latter. Among the materials studied, this empirical correlation is strong enough to suggest that the value of χ' can be a reliable indicator of network topology. This is of particular interest for amorphous solids, in which the bonding topology is an important structural issue[13,18–20] that must be decided on the basis of a variety of evidence.

In Sec. II we detail the present photoelastic model, and justify the assumptions involved. Section III describes how Table I was constructed. Section IV discusses the main result of this study, Fig. 4, and also develops the connection between bonding topology and photoelastic response. A summary, Sec. V, concludes the paper.

II. PHOTOELASTIC MODEL

The starting point of the present treatment is the Drude formalism and the Penn-Phillips single-oscillator model in which[10,11]

$$\epsilon_0 - 1 = \frac{4\pi\hbar^2 e^2}{m}\frac{NF}{VE_g^2} . \tag{2}$$

Here e and m are the electron charge and mass, N is the formal number of valence electrons per molecule participating in the oscillator, V is the corresponding molecular volume, and F is the oscillator strength appropriate to the Penn-Phillips model.[2,3] NF is then the effective number of electrons contributing to ϵ_0. The average gap E_g is defined by Eq. (2). The Penn-Phillips theory is preferred here, rather than alternative single-oscillator models (e.g., that proposed by Wemple and DiDomenico[21–23]), because it allows us to argue in favor of a small $d\ln F/d\ln V$ term, as a consequence of the f-sum rule. Differentiating Eq. (2) with respect to volume gives

$$\chi' = 1 - \frac{d\ln F}{d\ln V} + \frac{2}{E_g}\frac{dE_g}{d\ln V} . \tag{3}$$

A qualitative explanation has been suggested for the opposite signs of dE_t/dP and dn_0/dP in covalent solids with different network dimensionality.[24] This explanation can be easily understood on the basis of Eq. (3). Consider first Ge-family semiconductors. Because of their 3D-network structure, a macroscopic compression decreases the nearest-neighbor distance r, which in turn increases the bonding-antibonding interaction, and thereby increases E_g. The lower gaps, such as E_t, generally follow suit.[25,26] In this situation $dE_g/d\ln V<0$, and Eq. (3) implies $\chi'<1$. In fact, $\chi'<0$ for these covalent materials, so that n_0 decreases with pressure. The successful treatments of Van Vechten[2] and others[3] leave little doubt as to the validity of this approach for covalent 3D-network solids.

For molecular solids of network dimensionality less than 3, such as layered c-As_2S_3,[24] the situation is quite different. In this case, compression mainly forces the loosely bound molecular units closer

together without substantially changing the intramolecular distance r. Consequently, the bonding-antibonding interaction will not be strongly affected. Instead, the major change in electronic energies should derive from band broadening due to increased intermolecular overlap, so-called closed-shell interactions.[5] This can explain the observed negative dE_t/dP. One might also argue that n_0 should increase as the electronic threshold E_t is reduced. However, Eq. (3) fails to predict $\chi' > 1$ (the observed result), because we expect the average gap E_g to be nearly unaffected by pressure.[27]

Our approach to this dilemma is as follows. The molecular solids of interest here are all chalcogen based. For this class of solids, measurement shows that the valence electron contribution to the imaginary part of the dielectric function, $\epsilon_2(\omega)$, consists of two distinguishable regions.[28–30] The low- and high-energy regions, designated region I and region II, are generally believed to originate from transitions to antibonding states by nonbonding p-electrons (chalcogen lone-pair electrons) and bonding p-electrons, respectively.[31] However, the extent of hybridization is not necessarily small, as recently shown by Althaus *et al.* for c-As_2Se_3.[32]

To account for this dual structure in $\epsilon_2(\omega)$, a two-oscillator model will be adopted, with each oscillator of the Penn-Phillips type,

$$\epsilon_0 - 1 = (\epsilon_0 - 1)_{\mathrm{I}} + (\epsilon_0 - 1)_{\mathrm{II}} . \tag{4}$$

Here the left-hand side (the total $\epsilon_0 - 1$) is still given by Eq. (2) and

$$(\epsilon_0 - 1)_{\mathrm{I,II}} = \frac{4\pi\hbar^2 e^2}{m} \frac{n_{\mathrm{I,II}} f_{\mathrm{I,II}}}{V E_{\mathrm{I,II}}^2} , \tag{5}$$

where the subscripted quantities pertain to region I and region II. Following previous workers[5,7] we exclude nonbonding s-electrons from these regions; they are normally deep enough to be considered part of the core.[6]

Differentiating Eq. (4) with respect to volume and using Eq. (5) we find

$$\chi' = 1 - \frac{\chi_{\mathrm{I}}}{\chi} \frac{d\ln f_{\mathrm{I}}}{d\ln V} - \frac{\chi_{\mathrm{II}}}{\chi} \frac{d\ln f_{\mathrm{II}}}{d\ln V} + \frac{2}{E_g} \left[\frac{E_g}{E_{\mathrm{I}}} \frac{\chi_{\mathrm{I}}}{\chi} \right] \frac{dE_{\mathrm{I}}}{d\ln V} + \frac{2}{E_g} \left[\frac{E_g}{E_{\mathrm{II}}} \frac{\chi_{\mathrm{II}}}{\chi} \right] \frac{dE_{\mathrm{II}}}{d\ln V} , \tag{6}$$

where $\chi_{\mathrm{I,II}} = (\epsilon_0 - 1)_{\mathrm{I,II}}/4\pi$. According to the qualitative explanation outlined above,[5,24] the association of region II with bonding-antibonding transitions implies $dE_{\mathrm{II}}/d\ln V \approx 0$ for molecular solids; we shall neglect this term. Also the second and third right-hand terms will be combined and denoted by $-(d\ln f/d\ln V)^*$, the total effective oscillator strength contribution. Thus, we arrive at the analog of Eq. (3) for chalcogen-based molecular solids,

$$\chi' \approx 1 - \left[\frac{d\ln f}{d\ln V} \right]^* + \frac{2\eta}{E_g} \frac{dE_{\mathrm{I}}}{d\ln V} , \tag{7}$$

where $\eta = E_g \chi_{\mathrm{I}}/E_{\mathrm{I}}\chi$. The dimensionless parameter η is determined by the energies E_g, E_{I}, and E_{II}. Assuming insignificant interference from higher-lying transitions, we adopt the condition $NF = n_{\mathrm{I}} f_{\mathrm{I}} + n_{\mathrm{II}} f_{\mathrm{II}}$. Substituting this into Eqs. (2), (4), and (5) yields

$$\eta = \frac{E_g}{E_{\mathrm{I}}} \left[\frac{E_{\mathrm{II}}^2 - E_g^2}{E_{\mathrm{II}}^2 - E_{\mathrm{I}}^2} \right] . \tag{8}$$

Here $E_{\mathrm{II}} \geq E_g \geq E_{\mathrm{I}}$, so that $\eta > 0$. If a single-oscillator model is appropriate, viz., $E_{\mathrm{II}} = E_g = E_{\mathrm{I}}$, then $\eta = 1$, and Eq. (7) reduces to Eq. (3). With this convention, Eq. (7) can be used to treat both the Ge-family semiconductors, and the molecular chalcogenides.

The relative importance to ϵ_0 of regions I and II will be weighted toward lower energy because of the Kramers-Kronig relation

$$\epsilon_0 - 1 = (2/\pi) \int_0^\infty \epsilon_2(\omega)/\omega \, d\omega .$$

However, both terms in Eq. (4) must be included to preserve the f-sum rule, which requires

$$N \propto \int_0^\infty \omega \epsilon_2(\omega) d\omega ,$$

and thus emphasizes high-energy transitions.[23] In the limit $E_{\mathrm{II}} >> E_g \gtrsim E_{\mathrm{I}}$, we have $\chi_{\mathrm{I}}/\chi \approx 1$ and $2\eta/E_g \approx 2/E_{\mathrm{I}}$. Under these conditions Eq. (7) simulates a single-oscillator model for the electrons of region I. Many of the chalcogenide materials (except the IV–VI's) fall approximately into this category with $E_{\mathrm{II}} \gtrsim 2E_{\mathrm{I}}$. (See Table I below.)

The two-oscillator model has been considered previously for chalcogenide crystals and glasses. It was rejected in Ref. 5 because the ratio of bonding-antibonding to lone-pair oscillator energies ($E_{\mathrm{II}}/E_{\mathrm{I}}$ in the present notation) was assumed to be pressure independent. This assumption seems unrealistic because of the different bonding origin of

regions I and II, and because the measured $dE_t/d\ln V$ are large. Although we expect $dE_{II}/d\ln V \approx 0$, it seems unlikely that $dE_I/d\ln V \approx 0$ at the same time. In Ref. 7, the two-oscillator model was deemed unnecessary. Instead, for amorphous solids Eq. (3) was used, with connection made to E_t through the ansatz $d\ln E_t/dP = d\ln E_g/dP$. For chalcogenide glasses this also seems unrealistic, because it implies that higher-energy transitions shift faster than lower energy ones, i.e., a pressure-induced band narrowing not a band broadening. Furthermore, it would seem that higher-energy transitions should be associated with stronger bonds (as for E_{II}), and consequently tend to be less pressure sensitive than lower-energy transitions. For amorphous group IV and III–V solids the observation that $dE_t/dP < dE_g/dP$ may stem from the void structure of these materials.[4,33] We shall see that the photoelastic response of chalcogenide crystals and glasses can be described quite well by the two-oscillator model.

To summarize, the present treatment is based on the Drude formalism, the Penn-Phillips dielectric model, the experimental $\epsilon_2(\omega)$ indicating one oscillator for Ge-type and two oscillators for chalcogenide-based materials, and the assertion that $dE_{II}/d\ln V \approx 0$ in chalcogenide solids of network dimensionality less than 3.

III. CONSTRUCTION OF THE TABLE

To adequately test this model, it was necessary to compile data on a large number of materials. This is due both to the approximate nature of the model and the large variations found among the experimental photoelastic coefficients and band-gap pressure derivatives. An additional uncertainty derives from a lack of compressibility data for many of the thin film materials. In the following we discuss how the numbers in Table I were determined. Although experimental errors are generally not listed, the numbers have been rounded off such that the last significant figure can be expected to vary among different measurements. All tabulated substances are labeled either crystalline (c) or amorphous (a), except for the two crystalline forms of GeS_2. These are designated by their network dimensionality, either 2D (layered),[34] or 3D ("SiO_2"-like).[35] Of the other crystals having different polymorphic forms, c-S_8 refers to orthorhombic sulfur, c-Se and c-Te refer to the trigonal structures, c-SiO_2 is α-quartz, c-GeO_2 is the soluble hexagonal form, and the zinc chalcogenides are the sphalerite varieties. For further details and complete references, the reader should refer to the table footnotes.[36–66]

First of all, it was necessary to establish reliable values for E_g, which requires knowledge of N/V, F, and ϵ_0 [see Eq. (2)]. For the Ge family $N=8$ (two atoms per molecule for the elements); for the other substances all valence electrons were included, except nonbonding s electrons.[5,7] For example $N=(3\times2+4\times3)=18$ for As_2S_3, but $N=(4\times1+4\times2)=12$ for SiO_2. F has been shown to be $\sim\frac{2}{3}$ in tetrahedral semiconductors.[3] We have adopted this value throughout. The small variations in E_g that result from neglecting Van Vechten's A and D corrections,[2] are inconsequential for the present analysis. The density ρ (g/cm^3) is also listed in Table I; the sources include both x-ray and gravimetric measurements. For amorphous solids density is a nontrivial parameter, depending on the material fabrication process and the state of annealing. Variations of several percent are common in the literature, and some authors fail to mention the measured density of glasses used in their pressure studies. Consequently, the quoted densities represent typical values. Many of the tabulated ϵ_0 values come from the large compilations of Wemple *et al.*[21–23] They were obtained by fitting dispersion data using a Sellmeier oscillator scheme. Other sources include infrared optical constants, reststrahlen results, and measurements based on the frequency spacing of fringes seen in transmission. For a-GeS_2 the value in Ref. 62 seemed low, and an average with our own value was used.[42] ϵ_0 for a-GeO_2 was estimated by scaling (ϵ_0-1) of c-GeO_2 by $\rho(a\text{-}GeO_2)/\rho(c\text{-}GeO_2)$, assuming $E_g(c\text{-}GeO_2)$ unchanged, according to Eq. (2). The ϵ_0 and E_g values so obtained for a-GeO_2 are enclosed in parentheses.

The macroscopic compressibility K was obtained from experiment whenever possible. However, for many of the materials, especially those existing only as thin films, K is not known. In these cases K was estimated by an empirical rule which has been shown to hold for families of related crystalline and amorphous solids (e.g., for the As-Se system).[56] This rule relates the compressibilities $K(1)$ and $K(2)$ of two materials by

$$\frac{K(1)}{K(2)} \approx \left[\frac{\rho_{mol}(2)}{\rho_{mol}(1)}\right]^4, \tag{9}$$

where ρ_{mol} is the mean molecular density. K values for c-, a-GeS_2, and c-, a-$GeSe_2$ were obtained from $K(a\text{-Se})$; otherwise, K for an amorphous (crystalline) material was derived from its crystalline (amorphous) partner. Compressibilities so obtained appear in parentheses. The values seem quite reasonable.

For those materials where sufficient data exist, E_{I} and E_{II} were chosen to coincide with the peak positions in regions I and II of the experimental $\epsilon_2(\omega)$ spectra. For anisotropic crystals, a suitable average over polarization directions was used. E_{I} is generally close to the Sellmeier energy E_0, determined by Wemple.[22,23] Consequently, for c-S_8, which exhibits pronounced excitonic structure in $\epsilon_2(\omega)$,[67] we use $E_{\text{I}}=[E_0(\text{Wemple}^{23})]$. η for c-S_8 was then computed using the approximation $n_{\text{I}}f_{\text{I}}=\frac{1}{2}NF$, i.e., complete segregation of lone-pair and bonding electrons into regions I and II. For c-$GeSe_2$, E_{I} and E_{II} were determined by the two peaks in a model $\epsilon_2(\omega)$ spectrum (ϵ_2^A and ϵ_2^B in Fig. 5 of Ref. 30) that was deduced from ellipsometry data.[30] These energies were shifted downward by 0.3 eV for a-$GeSe_2$, according to the analysis of Ref. 30. E_{I} for 2D-GeS_2 and a-GeS_2 was estimated by scaling the c-$GeSe_2$ value by the appropriate ratio of threshold energies. For example,

$$E_{\text{I}}(\text{2D-GeS}_2)=E_{\text{I}}(c\text{-GeSe}_2)\frac{E_t(\text{2D-GeS}_2)}{E_t(c\text{-GeSe}_2)} .$$

η was then determined by requiring that $n_{\text{I}}f_{\text{I}}/NF$ have the c-$GeSe_2$ value. For 3D-GeS_2 the same procedure was followed, except that E_{I} for a-$GeSe_2$ was scaled, because of the similar photoelastic response of 3D-GeS_2 and a-$GeSe_2$. We found that the analysis was not sensitive to the exact convention chosen to establish E_{I} and E_{II}, as long as it reasonably placed these energies within regions I and II. Suitably defined moments of $\epsilon_2(\omega)$ would also suffice. However, our model is sensitive to the relative separations of E_{I}, E_g, and E_{II} through η [Eq. (8)].

For the molecular chalcogenides, the fraction of valence electrons contributing to region I is given by $n_{\text{I}}f_{\text{I}}/NF$. It is listed in the table, where appropriate. If the value for a substance was not obtained directly from the experimental E_{I} and E_{II} of that substance, it appears in parentheses. In such cases η was obtained from the relation $\eta=E_g^3 n_{\text{I}}f_{\text{I}}/E_{\text{I}}^3 NF$.

The tabulated band-gap volume derivatives are those available for the E_2 gap in the Ge-family materials[25] and for the E_t gap in the chalcogen-based solids. References cite the measured pressure coefficients which were subsequently divided by the appropriate compressibility. The literature was surveyed in order to select the most reasonable and reliable values. In many cases the quoted experimental error is less than the variation among different studies. Where two sources are referenced, their average is used. On the whole, an uncertainty of 30% is reasonable for these volume derivatives.

χ' characterizes the photoelastic response of the materials studied. For many of the cubic and isotropic solids, the quoted χ' were measured directly in hydrostatic pressure experiments, using various interference fringe techniques.[6,9,14,39,42] For anisotropic (and some cubic) substances, χ' was computed from appropriate averages of the photoelastic tensor components p_{ij}.[68] In general, one has

$$\chi'=\frac{\sum_{ij} p_{ij}e_j\epsilon_{0i}^2/(\epsilon_{0i}-1)}{3\sum_i e_i} , \tag{10}$$

where ϵ_{0i} and e_i are dielectric constant and strain components. Thus for cubic and amorphous solids

$$\chi'=\epsilon_0^2(p_{11}+2p_{12})/3(\epsilon_0-1) .$$

When the complete set of p_{ij} was not known, a suitable approximation was made. The table footnotes give greater detail. As for the band-gap coefficients, the available literature was surveyed to select the best values. Published experimental errors are again not included, because they are generally less than the variation among different measurements. Instead, to give the reader a realistic idea of the uncertainty in χ', all results deemed reasonable for a given material are listed. The most studied material seems to be a-As_2S_3, where the average of 7 measurements yields $\chi'_{\text{av}}=2.0\pm10\%$. The published[6] error is included for a-$GeSe_2$ to show that χ' is less than 1. Note that the overall uncertainty in χ' is consistent with the approximate nature of our model.

IV. DISCUSSION OF RESULTS

The solids under consideration fall into three groups, according to their χ' values. Ge-family solids exhibit $\chi'<0$, molecular chalcogenides display $\chi'>1$, and several group IV–VI compounds have $0\leq\chi'\leq1$. We now try to understand these empirical trends on the basis of Eq. (7). Our analysis points to a relationship between this classi-

TABLE I. Experimental photoelastic parameters χ' and band-gap pressure derivatives for 29 materials. All quantities necessary to test the model, i.e., Eq. (7) are also included.

Material	χ'	$\frac{dE_t}{d\ln V}$ (eV)	$\frac{dE_2}{d\ln V}$ (eV)	E_I (eV)	E_g (eV)	E_{II} (eV)	η	$\frac{n_I f_I}{NF}$	K (10^{-3} kbar^{-1})	ϵ_0	ρ (g/cm^3)	N
c-S_8	1.5[a]	0.5[o]		6.3[x]	6.97		0.7	(0.5)	13.0[a]	3.94[x]	2.07[qq]	32
	2.1[a]											
c-Se		2.4[p,f]		3.6[y]	4.28	8.3[y]	1.1	0.6	9.4[ee]	8.39[x]	4.82[ii]	8
a-Se	2.6[b]	1.6[q,r]		4.1[y]	5.08	8.0[y]	1.0	0.5	10.6[ff]	5.65[x]	4.28[ff]	8
c-Te	3.6[c]	3.9[s]		2.0[y]	2.2	8.3[y]	1.1	0.9	5.2[ee]	24.5[x]	6.25[ii]	8
a-Te				2.5[y]	2.9	7.2[y]	1.1	0.7	(6.9)[gg]	12.7[x]	5.82[pp]	8
c-As_2S_3		2.6[t]		4.2[z]	4.85	8.6[z]	1.0	0.7	(5.4)[gg]	7.00[x]	3.49[ii]	18
a-As_2S_3	1.9[d,e,f]	2.3[e]		4.9[z]	5.14	9.0[z]	1.0	0.9	7.79[hh]	5.89[x]	3.19[hh]	18
	2.0[d]											
	2.1[c]											
	2.2[g]											
	2.3[h]											
c-As_2Se_3		2.6[u,v]		3.3[z]	3.8	8.5[z]	1.1	0.7	(5.9)[gg]	9.7[kk]	4.80[ii]	18
a-As_2Se_3	2.4[f]	2.1[f,v]		3.9[z]	4.4	8.1[z]	1.0	0.7	6.96[ff]	7.1[kk]	4.60[ff]	18
2D-GeS_2	1.6[i]	1.6[i]		(4.8)[aa]	4.9		0.3	(0.3)[aa]	(5.6)[gg]	6.8[ll]	2.89[rr]	12
a-GeS_2	1.5[i]	3.1[i]		(4.5)[aa]	5.9		0.6	(0.3)[aa]	(7.4)[gg]	4.8[mm,i]	2.7[ss]	12
3D-GeS_2	1.0[i]	1.0[i]		(5.1)[bb]	7.0		1[dd]	(~0.02)[bb]	(4.9)[gg]	4.0[i]	2.99[tt]	12
							~0.05					
c-$GeSe_2$				3.5[cc]	4.7	5.6[cc]	0.7	0.3	(7.4)[gg]	7.0[cc]	4.56[ii]	12
a-$GeSe_2$	0.8±0.1[f]	0.9[f]		3.2[cc]	5.2	5.3[cc]	0.1	~0.02	(9.7)[gg]	5.5[nn]	4.26[uu]	12
c-SiO_2	0.89[j]				14.68		1		2.65[ii]	2.36[x]	2.65[u]	12
	0.95[j]											
a-SiO_2	0.84[h]				14.85		1		2.69[ii]	2.10[x]	2.20[ii]	12
	0.96[d]											
c-GeO_2					12.14		1		3.97[a]	2.82[x]	4.23[ii]	12
a-GeO_2	0.89[h]				(12.1)		1		(7.25)[gg]	(2.6)[oo]	3.64[ii]	12
c-Si	−0.7[k]		−2.8[w]		4.2		1		1.02[ii]	11.7[x]	2.34[ii]	8
	−0.3[l]											
a-Si	~−0.06[m]				3.78		1		(1.9)[gg]	12.0[x]	2.0[pp]	8
c-Ge	−2.3[d]		−4.2[w]		3.3		1		1.33[ii]	16.0[x]	5.32[ii]	8
	−1.6[k]											
	−1.1[k]											
a-Ge	−1.3[m]				3.1		1		(1.35)[gg]	17.4[x]	5.3[pp]	8
c-GaP	−1.1[c]				4.73		1		1.13[ii]	9.11[x]	4.13[ii]	8
	−0.6[m]											

TABLE I. *(Continued.)*

Material	χ'	$\frac{dE_t}{d\ln V}$ (eV)	$\frac{dE_2}{d\ln V}$ (eV)	E_I (eV)	E_g (eV)	E_{II} (eV)	η	$\frac{n_I f_I}{NF}$	K (10^{-3} kbar^{-1})	ϵ_0	ρ (g/cm^3)	N
a-GaP	−0.4[m]				4.0		1		(1.3)[gg]	12.0[pp]	4.0[vv]	8
c-GaAs	−1.2[k,m,n]				4.1		1		1.34[ii]	10.9[x]	5.4[ii]	8
a-GaAs	−0.8[m]				3.6		1		(1.8)[gg]	12.7[pp]	5.0[vv]	8
c-ZnS	−0.2[h]				6.75		1		1.28[ii]	5.07[x]	4.08[ii]	8
c-ZnSe	−0.5[d]				5.8		1		1.68[ii]	5.85[x]	5.3[ii]	8
	−0.2[d]											
c-ZnTe	−1.2[ww]				4.83		1		1.96[ii]	7.24[x]	6.34[ii]	8

[a]Reference 36 and references cited within; complete p_{ij} and/or c_{ij} (elastic constants) are known.
[b]Reference 37.
[c]Reference 38; for *c*-Te only p_{11} and p_{12} are known, and we used $\chi' \approx \epsilon_{av}^2(p_{11}+p_{12})/2(\epsilon_{av}-1)$.
[d]Reference 39.
[e]Reference 14.
[f]Reference 5.
[g]Reference 40.
[h]Reference 41.
[i]Reference 42; frequency spacing of fringes measured $n_0 d$ for one orientation under hydrostatic pressure.
[j]Reference 43; complete p_{ij} are known.
[k]Reference 44.
[l]Reference 45.
[m]Reference 4.
[n]Reference 46.
[o]Reference 47.
[p]Reference 48.
[q]Reference 49.
[r]Reference 50.
[s]Reference 51.
[t]Reference 52.
[u]Reference 53.
[v]Reference 54.
[w]Reference 25.
[x]Reference 23.
[y]Reference 28.
[z]Reference 29.
[aa]E_I obtained by scaling $E_I(c\text{-}GeSe_2)$; see text.
[bb]E_I obtained by scaling $E_I(a\text{-}GeSe_2)$; see text.
[cc]Reference 30.
[dd]Two values of η appear because $\chi'=1.0$ is a borderline case.
[ee]Reference 55.
[ff]Reference 56.
[gg]Derived from the empirical "law" of Ref. 56; see Eq. (9) and text of present work.
[hh]Reference 57.
[ii]Reference 58 and references cited within.
[jj]Reference 59 and references cited within.
[kk]Reference 60.
[ll]Reference 61.
[mm]Reference 62.
[nn]Reference 7.
[oo]Obtained from $\epsilon_0(c\text{-}GeO_2)$; see text.
[pp]Reference 22.
[qq]Reference 63.
[rr]Reference 34.
[ss]Reference 64.
[tt]Reference 35.
[uu]Reference 65.
[vv]Reference 66.
[ww]Present work.

fication scheme and network dimensionality.

Referring to Eq. (7), $\chi'=1$ is obtained if the pressure-induced change in ϵ_0 derives solely from a density increase. The condition $\chi' \gtrless 1$ is determined by the sign of the appropriate energy-gap volume derivative when $(d\ln f/d\ln V)^*$ can be neglected. According to the discussion in Sec. II, for the 3D-network Ge family we expect this coefficient (viz., $dE_g/d\ln V$) to be negative, corresponding to a compression-induced increase in the bonding-antibonding interaction. For the molecular chalcogenides, we anticipate that $dE_1/d\ln V$ will reflect pressure-induced band broadening in some way. The fact that $\chi'>1$ implies that $dE_1/d\ln V>0$. Although this is consistent with the sign of $dE_t/d\ln V$, a quantitative relationship between the pressure coefficients of the threshold and E_1 gaps is not apparent.

Our approach to this is empirical. Consider first the Ge-family semiconductors. It is well known that $dE_g/d\ln V$ is approximately the same for these materials.[25,26] The average measured coefficient for the E_2 gap is $(dE_2/d\ln V)_{\rm av}=-3.3\pm0.7$ eV, constant to within 20%, and negative. (E_2 is the optical gap most closely related to the Penn-Phillips E_g.[3] Data exist for c-Si, c-Ge, c-InSb, c-GaSb.[25]) Consequently, Eq. (7) predicts that χ' should exhibit an approximate linear dependence on $1/E_g$. This is indeed the case, and the extent of correlation can be seen in Fig. 4. This result is rather appealing. It implies [see Eq. (2)] that $(\chi'-1)$ scales as $(\chi V/N)^{1/2}$ [if $(d\ln f/d\ln V)^*$ is small].

It would be advantageous to preserve this simple scaling for the chalcogen-based solids. According to Eq. (7), χ' will depend linearly on η/E_g if $dE_1/d\ln V$ is constant. Although this coefficient has not been measured, Table I shows that $dE_t/d\ln V$ is roughly the same for those molecular chalcogenides with $\chi'>1$. For the nine such materials where data exist (excluding c-S_8, see below), $(dE_t/d\ln V)_{\rm av}=2.5\pm0.7$ eV, constant to 30%, and positive. Consequently, it seems reasonable to expect a similar material independence for $dE_1/d\ln V$, and we shall find this to be the case.

To test our model for both Ge-family and chalcogenide solids, and to discover the connection between $dE_t/d\ln V$ and $dE_1/d\ln V$, the following scheme was used. χ' was plotted against $2\eta/E_g$, with $\eta\equiv1$ when $\chi'<1$, and η given by Eq. (8) when $\chi'>1$. This plot is shown in Fig. 4. If Eq. (7) is indeed appropriate and $dE_g/d\ln V$ and $dE_1/d\ln V$ are approximately constant, we expect two straight lines, with slopes reflecting the average values of these energy-gap derivatives. The model's validity can then be judged by the extent of linear correlation and how closely the slopes compare to experimental coefficients. For Ge-family materials, the slope should be similar to $(dE_2/d\ln V)_{\rm av}$. For molecular chalcogenides, comparison of the $\chi'>1$ slope with $(dE_t/d\ln V)_{\rm av}$ should reveal the sought-after relation between $dE_t/d\ln V$ and $dE_1/d\ln V$. Our model is further judged by the reasonableness of this relation.

Eleven crystalline and amorphous Ge-family materials are plotted in Fig. 4. The extent of linear correlation is high—certainly within the experimental uncertainty defined by the spread in χ' values for a given substance (see for example, c-Ge, c-GaP, c-Si). The best-fit line for these $\chi'<0$ materials, forced to intersect $\chi'=1$ at $2\eta/E_g=0$ [viz., assuming $(d\ln f/d\ln V)^*\approx0$], has the slope -3.8 eV, nearly the same as -3.3 ± 0.7 eV (Ref. 25) for $(dE_2/d\ln V)_{\rm av}$. This agreement was to be expected on the basis of previous work.[2–4]

What is more surprising is that the degree of linear correlation is similar for molecular chalcogenides, having $\chi'>1$. Seven crystalline and amorphous materials of this type are plotted in Fig. 4. Again, the extent of linearity is well within the typical experimental uncertainty (see for example, a-As_2S_3 and c-S_8). A linear correlation would also result, but a weaker one, if we were to naively plot χ' versus $2/E_g$, as for a single oscillator [see Eqs. (3), (7), and (8)]. This is because $\eta\approx1$ for most of these substances (see Table I). However, we would then be forced to interpret the large positive slope as reflecting the value of $dE_g/d\ln V$. This would be incompatible with our expectation that the bonding-antibonding gap be insensitive to compression in a molecular solid. In fact, it would imply a substantial compression-induced *expansion* of the nearest-neighbor distance, a highly unlikely situation.[27] Only if $2/E_g$ is scaled by η are we justified in interpreting the positive $\chi'>1$ slope in Fig. 4 as giving $dE_1/d\ln V$. Again forcing the intercept to be at $\chi'=1$ [corresponding to $(d\ln f/d\ln V)^*\approx0$], the best-fit value of this slope is 2.7 eV. This is essentially the same as $(dE_t/d\ln V)_{\rm av}=2.5\pm0.7$ eV.

From these results we draw the following conclusions. The similar degree of linear correlation in Fig. 4, for Ge-family solids having $\chi'<0$ and molecular chalcogenides with $\chi'>1$, supports our model. The use of Eq. (7), with η given by Eq. (8) seems justified for both classes of solids. For the former group, a single-oscillator model is appropri-

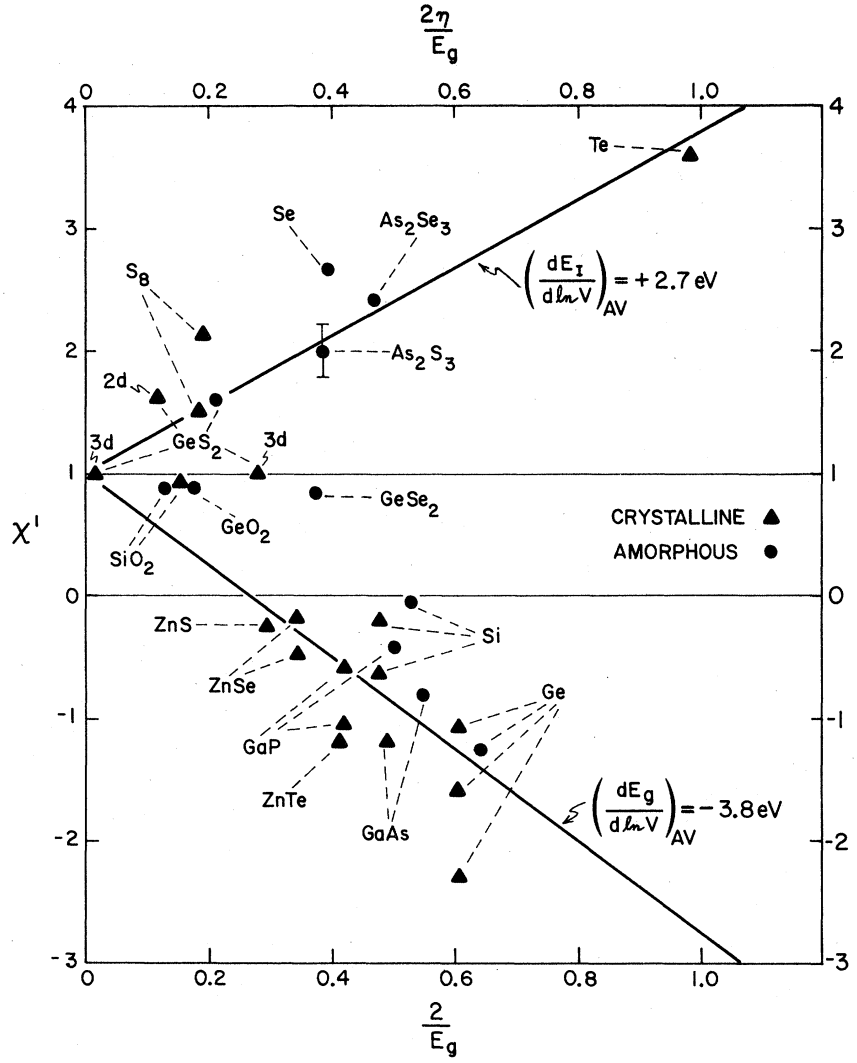

FIG. 4. Plot of experimental χ' versus $2\eta/E_g$, with $\eta \equiv 1$ for $\chi' < 1$ and η given by Eq. (8) for $\chi' > 1$. Triangles and dots denote crystalline and amorphous solids, respectively. Data scatter indicates experimental uncertainty in χ'; for a-As_2S_3, error bar shows the $\pm 10\%$ variation of seven different measurements. Points representing2D-GeS_2 and 3D-GeS_2 are labeled accordingly. 3D-GeS_2 is plotted twice ($\eta = 1$ and $\eta = 0.05$) because it falls on the $\chi' = 1$ border. $(dE_I/d\ln V)_{av} = 2.7$ eV and $(dE_g/d\ln V)_{av} = -3.8$ eV are the best linear fit slopes for $\chi' > 1$ and $\chi' < 0$ materials, respectively; intercepts at $\chi' = 1$ are forced. Materials with $0 \leq \chi' \leq 1$ are excluded from fits. See text for further interpretation.

ate, and the negative slope of χ' versus $2/E_g$ reflects $dE_g/d\ln V$. Compression mainly increases the bonding-antibonding gap at the rate $(dE_g/d\ln V)_{av} = -3.8$ eV, which is roughly material independent within the Ge family. For the $\chi' > 1$ molecular chalcogenides, a two-oscillator model is appropriate, with $dE_{II}/d\ln V << dE_I/d\ln V$. The positive slope of χ' versus $2\eta/E_g$ reflects $dE_I/d\ln V$. This coefficient is $(dE_I/d\ln V)_{av} = 2.7$ eV, approximately equal to the coefficient for the threshold gap, both of which are largely material independent. Although for a given given chalcogenide crystal the volume derivatives of specific gaps may vary,[5,6] as they do for Ge-family crystals,[25] on the average compression causes a uniform red shift of region I while region II remains stationary. Thus, for these molecular chalcogenides, the expected pressure-induced band

broadening is manifest in the photoelastic response through the increased separation of $E_{\rm I}$ and $E_{\rm II}$.

These conclusions can be related to bonding topology, by considering the analogy to the pressure dependence of optical phonons in solids having different network dimensionality. The effect of compression on a phonon of frequency ν_i is characterized by its mode Grüneisen parameter $\gamma_i = -d\ln\nu_i/d\ln V$. For the Ge family, optical phonons exhibit $\gamma_i \sim 1$.[69] This value reflects the nearest-neighbor bond compression Δr, which, because of the isotropic 3D network, is related to the macroscopic ΔV by $3\Delta r/r = \Delta V/V$. For chalcogen-based molecular solids, a single γ_i is not appropriate. High-frequency (internal) modes are much less sensitive to compression than low-frequency (external) vibrations; in fact one can have $(\gamma_{\rm int}/\gamma_{\rm ext}) \sim (1/100)$.[70–72] The detailed relationship of this result to the large bonding-strength dichotomy in low (<3D)-network dimensionality solids was explained by Zallen.[70] In essence, the stiff nearest-neighbor bonds that form the covalent (<3D)-network are "insulated" from compression by the soft intermolecular (i.e., internetwork) forces. The latter bear the brunt of the macroscopic volume change. Zallen proposed, and supported with extensive high-pressure Raman data,[52,70,71,73] a scaling law in which $\gamma_i \propto \nu_i^{-2} \propto k_i^{-1}$. Here k_i is the force constant for mode i.

This picture of the response of phonons to pressure has definite implications for electronic transitions. For the 3D-network Ge family, E_g should increase strongly in response to the negative Δr. Therefore [from Eq. (3) or (7)] $\chi' < 1$, and in fact $dE_g/d\ln V$ is always large enough so that $\chi' < 0$. For the (<3D)-network molecular chalcogenides, the association of $E_{\rm II}$ with bonding-antibonding transitions implies that $dE_{\rm II}/d\ln V$ is small because Δr is small. In contrast, the association of $E_{\rm I}$ with transitions from states having substantial nonbonding (lone-pair) character implies $dE_{\rm I}/d\ln V$ is large. This is because nonbonding electrons are located with greatest probability in the highly compressible intermolecular (internetwork) volume away from the bonds.[5] Although the $\chi' > 1$ and $\chi' < 1$ slopes in Fig. 4 suggest that $dE_{\rm I}/d\ln V$ and $dE_{\rm II}/d\ln V$ would have similar magnitudes if the *macroscopic* compression were equally applied, the bonding-strength dichotomy does not permit this. One can write

$$dE_{\rm I,II}/d\ln V = (dE_{\rm I,II}/d\ln V_{\rm I,II}) \times (K_{\rm I,II}/K) ,$$

where $K_{\rm I}$ and $K_{\rm II}$ denote the *microscopic* compressibilities of the intermolecular volume $V_{\rm I}$ and the intramolecular volume $V_{\rm II}$. Thus, using $|dE_{\rm I}/d\ln V_{\rm I}| \approx |dE_{\rm II}/d\ln V_{\rm II}|$ and the results of Refs. 70–72, we estimate

$$\left|\frac{dE_{\rm II}}{d\ln V}\right| \Big/ \left|\frac{dE_{\rm I}}{d\ln V}\right| \approx \frac{K_{\rm II}}{K_{\rm I}} \approx \frac{k_{\rm ext}}{k_{\rm int}} \sim 10^{-2} , \tag{11}$$

where $k_{\rm ext}$ and $k_{\rm int}$ are typical force constants for external and internal vibrations. This justifies retaining only the term in $dE_{\rm I}/d\ln V$ in Eq. (7). Furthermore, we expect $dE_{\rm I}/d\ln V$ to reflect any compression-induced band broadening, because nonbonding electrons, by virtue of their location, should be most susceptible to increased intermolecular overlap. Even in cases where substantial hybridization is likely, e.g., c-As_2Se_3,[32] it appears that the effects of compression are dominated by the principal location of the electrons, either in the inter- or intramolecular volume. Since the data show that band-broadening occurs through a uniform red shift of region I with respect to a stationary region II, $dE_{\rm I}/d\ln V$ is large and positive and $\chi' > 1$.

In this way, the observed photoelastic trends can be related to bonding topology. We suggest that the correlations in Fig. 4 are sufficient for χ' to be used as a handy indicator. $\chi' < 0$ implies a covalent 3D-network solid, and $\chi' > 1$ implies a solid of covalent network dimensionality less than 3.

A third category is formed by materials having $0 \le \chi' \le 1$. This group contains the more ionic alkali halides,[1,2] and many hybrid composition group IV–VI solids. Within the present model there are two[74] probable ways to realize $0 \le \chi' \le 1$. Referring to Eq. (6), if $dE_{\rm I}/d\ln V = dE_{\rm II}/d\ln V = 0$, then the only contribution to χ' is the density increase term, and $\chi' = 1$. This may approximate the situation in alkali halides. However, band-gap changes are not negligible in alkali halides because χ', though positive, is less than 1.[1,2] The second possibility is that the terms containing $dE_{\rm I}/d\ln V$ and $dE_{\rm II}/d\ln V$ in Eq. (6) are comparable, but of opposite sign. Their cancellation would again make the density term dominant. This type of fortuitous cancellation is perhaps more likely in c-$GeSe_2$, a-$GeSe_2$, and 3D-GeS_2, for which experiment indicates two oscillators of similar strengths.[30] However for these materials, as well as SiO_2 and GeO_2, the role of ionicity should not be ignored.

It seems somewhat anomalous that a-$GeSe_2$ has $\chi' < 1$ while a-GeS_2 is firmly in the (<3D)-network

molecular class, with $\chi'=1.5$.[42] A recent structural model of both glasses places them in the molecular group, with locally layerlike "outrigger rafts" forming topologically one-dimensional units.[18–20] Since the bona fide layer crystal 2D-GeS_2 has $\chi'=1.6$, the a-GeS_2 result appears normal. However, $\chi'=0.8\pm0.1$[5] for a-$GeSe_2$ is closer to $\chi'=1.0$ for 3D-GeS_2, which sits on the borderline of our classification scheme. [Accordingly, χ' (3D-GeS_2) is plotted against both $2/E_g$ and $2\eta/E_g$ in Fig. 4.] We conclude that the present situation for materials with $0\leq\chi'\leq1$ is ambiguous. A strict correlation of χ' with network dimensionality may not be realistic, especially for complicated structures such as 3D-GeS_2.[42]

Finally, we note the case of c-S_8. A Lorenz-Lorentz treatment may be more appropriate here, because the S_8 rings of this *0D-network* [12] solid do not have macroscopic extent. The value of χ' so obtained [using $\chi'=(\epsilon_0+2)/3$][5] is $\chi'=2.0$, in good agreement with experiment. For this reason we excluded c-S_8 when computing $(dE_t/d\ln V)_{av}$ for $\chi'>1$ materials.

V. SUMMARY

The different photoelastic response of Ge family and chalcogen-based molecular solids was investigated. This difference is reflected in the sign and magnitude of the susceptibility Grüneisen coefficient χ'. New data to 80 kbar were also presented for c-ZnTe.

Within the Drude formalism, ϵ_0 was approximated by one Penn-Phillips oscillator for the Ge family, and two such oscillators (with strengths determined from experiment) for the molecular chalcogenides. Our largely empirical approach was guided by the experimental $\epsilon_2(\omega)$ spectra. An additional rationale for the two-oscillator model is the presence of both bonding and nonbonding electrons in chalcogenide solids. An expression [Eq. (7)] for χ' was obtained that is applicable to *both* groups of materials. This expression predicts a linear dependence of χ' on $2\eta/E_g$, given the approximate material invariance of measured band-gap volume derivatives. The $\chi'\gtrless1$ slopes of this dependence should yield $dE_g/d\ln V$ for the Ge family ($\eta\equiv1$), and $dE_I/d\ln V$ for molecular chalcogenides.

The quantities needed to test our model were tabulated for 29 materials of interest. The literature was surveyed to obtain the best values. Unmeasured compressibilities were estimated from density ratios by an empirical law connecting related materials. The experimental $dE_2/d\ln V$ for the Ge family, and $dE_t/d\ln V$ for the chalogenides, were included for comparison with the slopes in the χ' versus $2\eta/E_g$ plot. The materials divide into three classes according to their χ' values. The Ge-family substances have $\chi'<0$, whereas the molecular chalcogenides (save perhaps a-$GeSe_2$) have $\chi'>1$. Several group IV–VI hybrids have $0\leq\chi'\leq1$, a regime known to apply also to alkali halides.

A plot of χ' versus $2\eta/E_g$ was constructed, with $\eta\equiv1$ for $\chi'<1$, and η given by Eq. (8) for $\chi'>1$. As predicted, two linear correlations were found; their slopes were in excellent agreement with the measured $(dE_g/d\ln V)_{av}$ for $\chi'<0$ materials, and with $(dE_t/d\ln V)_{av}$ for $\chi'>1$ solids. The observed linear dependences applied equally well to both crystalline and amorphous materials. These results constitute definite evidence in support of our model. In addition, we find that the band broadening expected for *molecular* chalcogenides is manifest through a uniform red shift of oscillator I, viz., $dE_I/d\ln V\approx(dE_t/d\ln V)_{av}>0$, with respect to a stationary oscillator II, viz., $dE_{II}/d\ln V\approx0$.

An argument was put forward relating the observed photoelastic trends to network dimensionality. Ge-family materials have $\chi'<0$ because their 3D-network structure allows the macroscopic compression to be completely transferred to covalent-bond reduction. This is not possible for the molecular chalcogenides because their ($<3D$) networks introduce vastly different microscopic compressibilities for intramolecular and intermolecular volumes. This situation for electronic transitions is analogous to that for phonons.[70,71] In both cases, and for the same reasons, high-energy excitations are much less sensitive to compression than low-energy ones. The relative sensitivities should scale as the ratio of intra- to intermolecular force constants, which can be as low as $\sim10^{-2}$ in molecular chalcogenides. The strong effect of overlap on electrons located in the intermolecular volume explains $dE_I/d\ln V>0$. Finally, it was suggested that χ' should be a reliable indicator of bonding topology, viz., $\chi'<0$ for covalent 3D-network solids, and $\chi'>1$ for ($<$ 3D)-network structures. However, this correlation does not appear to extend to $0\leq\chi'\leq1$ materials for which the present situation seems ambiguous.

*Present address: Stanford University, Department of Physics, Stanford, Ca. 94305.
[1]K. Vedam and S. Ramaseshan, in *Progress in Crystal Physics,* edited by R. S. Krishnan (Wiley, New York, 1958), Vol. I, p. 102; T. S. Narasimhamurty, *Photoelastic and Electro-Optic Properties of Crystals* (Plenum, New York, 1981), pp. 290–293.
[2]J. A. Van Vechten, Phys. Rev. 182, 891 (1969).
[3]M. Cardona, *Atomic Structure and Properties of Solids,* Proceedings of the International School of Physics "Enrico Fermi", Course LII, edited by E. Burstein (Academic, New York, 1972), p. 514.
[4]G. A. N. Connell and W. Paul, J. Non-Cryst. Solids 8–10, 215 (1972).
[5]M. Kastner, Phys. Rev. B 6, 2273 (1972); 7, 5237 (1973); M. Kastner and R. R. Forberg, Phys. Rev. Lett. 36, 740 (1976).
[6]H. Wendel, R. M. Martin, and D. J. Chadi, Phys. Rev. Lett. 38, 656 (1977); J. D. Joannopoulos, Th. Starkloff, and M. Kastner, *ibid.* 38, 660 (1977).
[7]G. Lucovsky, Phys. Rev. B 15, 5762 (1977).
[8]H. Mueller, Phys. Rev. 47, 947 (1935).
[9]K. Vedam and E. D. D. Schmidt, Phys. Rev. 146, 548 (1966).
[10]D. Penn, Phys. Rev. 128, 2093 (1962).
[11]J. C. Phillips, Rev. Mod. Phys. 49, 317 (1970).
[12]R. Zallen, in *Proceedings of the 12th International Conference on the Physics of Semiconductors, Stuttgart, 1974,* edited by M. H. Pilkuhn (Teubner, Stuttgart, 1974), p. 621.
[13]R. Zallen, *The Physics of Amorphous Solids* (Wiley, New York, to be published).
[14]B. A. Weinstein, R. Zallen, and M. L. Slade, J. Non-Cryst. Solids 35,36, 1255 (1980).
[15]J. M. Besson, J. Cernogora, M. L. Slade, B. A. Weinstein and R. Zallen, Physica 105B, 319 (1981).
[16]G. J. Piermarini and S. Block, Rev. Sci. Instrum. 46, 973 (1975).
[17]D. Langer, in *Proceedings of the 7th International Conference on the Physics of Semiconductors,* edited by M. Hulin (Dunod, Paris, 1964), p. 241.
[18]J. C. Phillips, J. Non-Cryst. Solids 34, 153 (1979); 43, 37 (1981).
[19]P. M. Bridenbaugh, G. P. Espinosa, J. E. Griffiths, J. C. Phillips, and J. P. Remeika, Phys. Rev. B 20, 4140 (1979).
[20]J. C. Phillips, C. A. Beevers, and S. E. B. Gould, Phys. Rev. B 21, 5724 (1980).
[21]S. H. Wemple and M. DiDomenico, Jr., Phys. Rev. B 3, 1338 (1971).
[22]S. H. Wemple, Phys. Rev. B 7, 3767 (1973).
[23]S. H. Wemple, J. Chem. Phys. 67, 2151 (1977).
[24]R. Zallen and D. F. Blossey, *Optical and Electrical Properties of Compounds with Layered Structures,* edited by P. A. Lee (Reidel, Dordrecht, 1976), p. 231.
[25]R. Zallen and W. Paul, Phys. Rev. 155, 703 (1967).
[26]P. J. Meltz, J. Phys. Chem. Solids 28, 1441 (1967).
[27]For molecular solids, any slight compression of r should show up as an increase in the bonding-antibonding gap, as for Ge-family materials. Sometimes, as for Se and Te, hydrostatic compression actually *increases* r slightly. In any case, the resulting bonding-antibonding energy change is generally *small.*
[28]J. Stuke, J. Non-Cryst. Solids 4, 1 (1970).
[29]R. E. Drews, R. L. Emerald, M. L. Slade, and R. Zallen, Solid State Commun. 10, 293 (1972).
[30]D. E. Aspnes, J. C. Phillips, K. L. Tai, and P. M. Bridenbaugh, Phys. Rev. B 23, 816 (1981).
[31]M. Kastner, Phys. Rev. Lett. 28, 355 (1972).
[32]H. L. Althaus, G. Weiser, and S. Nagel, Phys. Status Solidi B 87, 117 (1978).
[33]B. A. Weinstein, Phys. Rev. B 23, 787 (1981).
[34]G. Dittmar and H. Schafer, Acta Crystallogr. B31, 2060 (1975).
[35]G. Dittmar and H. Schafer, Acta Crystallogr. B32, 1188 (1976).
[36]R. F. S. Hearmon and D. F. Nelson, *Landolt-Bornstein, New Series, group III, Vol. II, Elastic, Piezoelectric and Related Constants of Crystals,* edited by K.-H. Hellwege and A. M. Hellwege (Springer, Berlin, 1979), pp. 495–551.
[37]W. C. Schneider and K. Vedam, J. Opt. Soc. Am. 60, 800 (1970).
[38]R. W. Dixon, J. Appl. Phys. 38, 5149 (1967).
[39]A. Feldman, D. Horowitz, R. W. Waxler, and M. J. Dodge, in NBS Technical Note 993, *Optical Materials Characterization,* (U. S. Government Printing Office, Washington, 1979), pp. 56–63.
[40]R. K. Galkiewicz and J. Tauc, Solid State Commun. 10, 1261 (1972).
[41]R. M. Waxler, IEEE J. Quantum Electron. QE-7, 166 (1971).
[42]B. A. Weinstein, R. Zallen, and M. L. Slade Phys. Rev. B (in press).
[43]T. S. Narasimhamurty, J. Opt. Soc. Am. 59, 682 (1969).
[44]M. Cardona and F. H. Pollak, in *The Physics of Opto-Electronic Materials,* edited by W. A. Albers, Jr. (Plenum, New York, 1971), p. 81.
[45]D. K. Biegelsen, Phys. Rev. Lett. 32, 1196 (1974).
[46]D. K. Biegelsen, J. C. Zesch, and C. Schwab, Phys. Rev. B 14, 3578 (1976).
[47]H. G. Drickamer, in *Solid State Physics,* edited by F. Seitz and D. Turnbull (Academic, New York, 1965), Vol. 17, pp. 38–43.
[48]V. Y. Krisciunas, M. P. Mikalkevicius, and A. Yu Shileika, Fiz. Tverd. Tela (Leningrad) 7, 2571 (1965) [Sov. Phys.—Solid State 7, 2080 (1966)].
[49]R. S. Caldwell and H. Y. Fan, Phys. Rev. 114, 664 (1959).
[50]W. Fuhs, P. Schlotter, and J. Stuke, Phys. Status Solidi B 57, 587 (1973).
[51]Yu. V. Kosichkin, in *The Physics of Selenium and Tellurium,* edited by E. Gerlach and P. Grosse (Springer, Berlin, 1979), p. 96.
[52]J. M. Besson, J. Cernogora, and R. Zallen, Phys. Rev.

B 22, 3866 (1980).
[53]A. J. Grant and A. D. Yoffe, Solid State Commun. 8, 1919 (1970).
[54]B. T. Kolomiets and E. M. Raspopova, Fiz. Tekh. Poluprovodn. 4, 157 (1970) [Sov. Phys.—Semicond. 4, 124 (1970)].
[55]T. A. Fjeldly and W. Richter, Phys. Status Solidi B 72, 555 (1975); R. M. Martin, T. A. Fjeldly, and W. Richter, Solid State Commun. 18, 865 (1976); L. F. Vereshchagin, S. S. Kabalkina, and B. M. Shulenin, Doklady Akad. Nauk. SSSR 165, 297 (1965). [Sov. Phys. Dokl. 10, 1053 (1966)].
[56]N. Soga, M. Kunugi, and R. Ota, J. Phys. Chem. Solids 34, 2143 (1973).
[57]D. Gerlich, E. Litov, and O. L. Anderson, Phys. Rev. B 20, 2529 (1979).
[58]*Comprehensive Inorganic Chemistry,* edited by J. C. Bailar, Jr., H. J. Emeleus, Sir R. Nyholm, and A. F. Trotman-Dickenson (Pergamon, Oxford, 1973), Vols. 1–3.
[59]R. M. Martin, Phys. Rev. B 1, 4005 (1970).
[60]R. Zallen, R. E. Drews, R. L. Emerald, and M. L. Slade (unpublished).
[61]P. M. Nikolic and Z. V. Popovic, J. Phys. C 12, 1151 (1979).
[62]G. Lucovsky, J. P. deNeufville, and F. L. Galeener, Phys. Rev. B 9, 1591 (1974).
[63]*CRC Handbook of Chemistry and Physics,* 61st Edition, edited by R. C. Weast and M. J. Astle (CRC Press, Boca Raton, 1980), pp. B73–B166.
[64]L. Cervinka and A. Hruby, in *Proceedings of the 5th International Conference on Liquid and Amorphous Semiconductors,* edited by J. Stuke and W. Brenig (Taylor and Francis, London, 1974), p. 431.
[65]R. Azoulay, H. Thibierge, and A. Brenac, J. Non-Cryst. Solids 18, 33 (1975).
[66]J. Stuke and G. Zimmerer, Phys. Status Solidi B 49, 513 (1972).
[67]R. L. Emerald, R. E. Drews and R. Zallen, Phys. Rev. B 14, 808 (1976).
[68]See, for example, J. F. Nye, *Physical Properties of Crystals* (Clarendon, Oxford, 1967).
[69]B. A. Weinstein and G. J. Piermarini, Phys. Rev. B 12, 1172 (1975).
[70]R. Zallen, Phys. Rev. B 9, 4485 (1974).
[71]R. Zallen and M. L. Slade, Phys. Rev. B 18, 5775 (1978).
[72]T. Chattopadhyay, C. Carlone, A. Jayaraman, and H. G. v. Schnering, Phys. Rev. B 23, 2471 (1981).
[73]M. L. Slade, R. Zallen, and B. A. Weinstein, (unpublished).
[74]$0 \leq \chi' \leq 1$ could also be achieved by cancellations involving large oscillator strength changes, i.e., $(d\ln f/d\ln V)^*$. However, this seems less likely to us.